Parallel 2D-RF excitation for arbitrarily shaped region–of-interest MR spectroscopy at 16.4 T

Dinesh K Deelchand[1], Xiaoping Wu[1], Pierre-Gilles Henry[1], and Pierre-Francois Van de Moortele[1]
[1]*Center for Magnetic Resonance Research, University of Minnesota, Minneapolis, MN, United States*

Introduction: MR spectroscopy (MRS) greatly benefits from higher magnetic fields due to increased SNR and spectral resolution. Most single-voxel MRS sequences select cubic voxels that cannot match the shape of anatomical structures of interest, leading to partial volume effects and/or reduced SNR. On the other hand, 2D-RF excitation pulses have the potential to selectively excite arbitrarily shaped region-of-interest (ROI) [1-5]. However, a critical issue with 2D-RF pulses for MRS consists in preserving the necessary bandwidth (BW_{min}) to cover the metabolites of interest (typically from 0.5 to 4.2 ppm) and to limit chemical shift displacement (CSD). As BW_{min} increases linearly with B_0, 2D-RF pulse design also becomes harder at high field. Recently developed parallel excitation (pTX) methods, however, provide new means to mitigate or work around these obstacles. The purpose of this work is 1) to demonstrate the feasibility of achieving arbitrarily shaped 2D-RF pulse excitation at a very high field (16.4 T) while 2) preserving sufficient bandwidth for ^{1}H MRS (~4ppm) and 3) taking advantage of parallel RF excitation capability with a 2-channel RF coil. Furthermore, using a segmented radial k-space trajectory we also 4) introduce a novel, segment-wise simulation guided RF pulse design to correct for gradient waveform deviations.

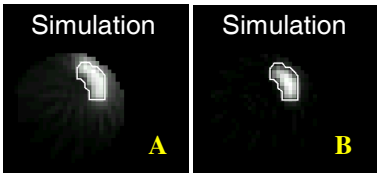

Figure 1: Simulated excitation patterns with two RF pulse design methods: (A) whole k-space RF pulse design split into segments (B) RF pulse designed using individual measured GW for each segment. The solid line delineates the target ROI. Using the same color scale, side excitation pattern outside the ROI seen in (A) vanish in (B).

General Methods: Experiments were conducted on 16.4 T horizontal bore system (Agilent, USA) interfaced to a DirectDrive console with 4 independent transmit and receive channels. A two-channel RF coil was used (each element used as transceiver) with a phantom containing 50 mM GABA and a bean-shaped ROI was chosen for RF pulse design (Fig.3). To limit the impact of ΔB_0, B_0 shim was done over a larger ROI using FASTMAP until water linewidth < 10 Hz. Absolute B_1^+ maps for each individual coil were measured using the 3D AFI technique [6].

MR sequence, RF Pulse design and Results: Segmented radial k-space trajectories have been shown to offer intrinsic advantages for 2D-RF pulse in MRS, including a higher sampling density in central k-space [1,5]. We used an N-spoke (N=20) spin-echo segmented radial k-space (Fig. 2) running 1 excitation spoke at a time (a spoke travels forth and back between k-space center and periphery) to maximize spectral BW (here BW is limited by gradient strength and slew rate) and minimize spatial CSD. After the collection of N complex signals, the latter are averaged to form the ROI-selective MR signal.

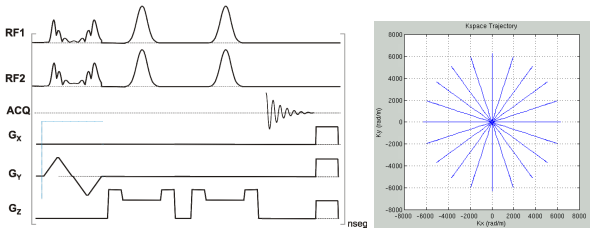

Figure 2: N-segments (N=20) spin-echo radial sequence. For each segment the sequence includes: VAPOR water suppression (not shown), 1 spoke out of N of the 2-channel 2D-RF pulse, a pair of slice-selective adiabatic refocusing pulse, signal acquisition followed by gradient spoilers.

The 2D-RF pulses were designed in the small flip-angle (FA) regime using the spatial domain method [7] to achieve 10° excitation in the ROI. To minimize errors in pTX excitation pattern due to gradient waveform (GW) imperfections [8], we measured the actual k-space trajectories [9]. It has been proposed to first design one RF pulse covering the whole k-space then split the latter into individual segments [1-5]. However, this may result in severe side excitation outside the ROI as shown in Fig.1A. Here, we introduce a new approach: one RF pulse covering the whole k-space is initially designed based on nominal k-space trajectories and is then split into individual segments. The segmented pulses are fed to a Bloch simulator to compute the target excitation pattern for each segment, and corresponding segment-wise RF pulses are re-designed using the measured segmented GW. As seen in Fig.1, the simulated excitation pattern using our proposed method (Fig.1B) is far more accurate than the single pulse approach (Fig.1A). Experimental results (Fig.3) are fully consistent with simulations, with minimal levels of side excitation outside the target ROI, together with satisfactory spectral quality. The shape and location of the excitation patterns were well preserved for up to 3 kHz offset although, as expected, the intensities were reduced at the edges of the frequency offset window (Fig.3).

Discussion: Our results demonstrate that even at 16.4 T, 2D-RF shaped pulses can be used while preserving satisfactory BW for ^{1}H MRS. Even though radial k-space sequences provide higher SNR than in Cartesian grids, they also require a larger number (+ ~57%) of excitations. However, multi-transmit RF design can be used to substantially reduce N. In the case presented here, using N=20 spokes with a 2-coil RF design provided the same pattern accuracy as using N=30 spokes but with the two coils combined in fixed, single channel quadrature mode. Furthermore, pTX resources can be used in other ways: reducing N to shorten acquisition time or to reduce sensitivity to motion, reducing RF power demands for a given pattern accuracy, improving excitation pattern and reduce side excitation for a given number of spokes, etc. Although in this preliminary work a small FA pulse design was considered, other algorithms such as optimal control can be used to achieve larger FA [10], which is essential for MRS acquisitions.

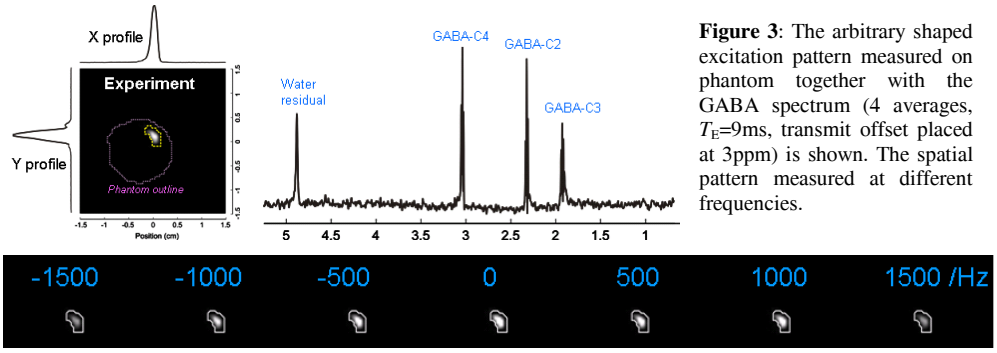

Figure 3: The arbitrary shaped excitation pattern measured on phantom together with the GABA spectrum (4 averages, T_E=9ms, transmit offset placed at 3ppm) is shown. The spatial pattern measured at different frequencies.

References: [1] Qin MRM 2007; [2] Weber-Fahr MRI 2009; [2] Finsterbusch MRM 2011; [3] Busch MRM 2011; [5] Snyder MRM 2011; [6] Yarnykh MRM 2007; [7] Grissom MRM 2006; [8] Wu MRM 2010; [9] Duyn JMR 1998; [10] Conolly IEEE TMI 1986.

Acknowledgement: This work was supported by fundings from P41 EB015894, P30 NS057091, P30 NS076408 and S10 RR025031.